Available online at www.sciencedirect.com
SCIENCE DIRECT
Journal of Organometallic Chemistry 691 (2006) 907–915
Journal of Organometallic Chemistry
www.elsevier.com/locate/jorganchem

HMB and Cp* ruthenium(II) complexes containing bis- and tris-(mercaptomethimazolyl)borate ligands: Synthetic, X-ray structural and electrochemical studies (HMB = η^6-C_6Me_6, Cp* = η^5-C_5Me_5)

Seah Ling Kuan [a], Weng Kee Leong [a], Lai Yoong Goh [a,*], Richard D. Webster [b]

[a] Department of Chemistry, National University of Singapore, Kent Ridge, Singapore 119260, Singapore
[b] Research School of Chemistry, Australian National University, Canberra, ACT 0200, Australia

Received 7 September 2005; received in revised form 7 October 2005; accepted 21 October 2005
Available online 5 December 2005

Abstract

The reactions of $[(HMB)RuCl_2]_2$ with $K[HB(mt)_3]$ and $Na[H_2B(mt)_2]$ (mt = *N*-methyl-2-mercaptoimidazol-1-yl) led to the isolation of $[(HMB)Ru\{HB(mt)_3\}]Cl$ (**1**) (ca. 66% yield) and $[(HMB)Ru\{H_2B(mt)_2\}]Cl$ (**2**) (ca. 70% yield), respectively. The reaction of $[Cp^*Ru\text{-}OMe]_2$ with $Na[H_2B(mt)_2]$ yielded $Cp^*Ru[H_2B(mt)_2]$ (**3**) (ca. 85% yield). Single crystal X-ray diffraction analyses were carried out on all three complexes, together with cyclic voltammetric measurements.

Keywords: Cp*/(HMB)ruthenium; (Mercaptomethimazolyl)borate; Structures; Electrochemistry; Scorpionate

1. Introduction

Since its first reported synthesis, the tris(methimazolyl)-borate anion, $HB(mt^R)_3^-$ (also abbreviated as Tm^R) (mt = *N*-methyl-2-mercaptoimidazol-1-yl) [1],the S_3-donor soft analogues of Trofimenko's versatile N_3-donor poly(pyrazolyl)borates, $HB(pz)_3^-$ (also abbreviated as Tp^R) [2] (Chart 1) has attracted an intense interest. Its coordination chemistry and that of the allied ligand $H_2B(mt^R)_2$ (also abbreviated as Bm^R) [3] has been rapidly developing in several laboratories; to date complexes of types M(Tm) [4], $M(Tm)_2$ and $M(Bm)_2$ [4f,5] and [M(Tm)X] [X = Cl, Br, I] [5d,6] of first row transition metals of Groups 8–10, of Groups 11 and 12 metals and of the main group elements Tl, Sn, Pb, As and Bi, have been prepared.

Alongside this development, the organometallic chemistry of this class of soft scorpionate ligands was also emerging. Among the organometallic examples to date were complexes containing alkyl tin halides [7], metal carbonyls, which include $(Tm)Mo(CO)_2(\eta^3\text{-allyl})$ and $(Tm)W(CO)_3I$ [4e] and $(Bm^R/Tm^R)Mn(CO)_3$ [8], the anionic species $[(Tm)Mo(CO)_3]^-$and$[(Bm)Mo(CO)_4]^-$ [9], and alkylidyne complexes $(Tm)W(\equiv CR)(CO)_2$ [10], and those of pharmaceutical interest, viz. *fac*-$(Bm/Tm)M(CO)_3$ (M = Tc and Re) [11]. After a first example in 1999, Hill had since synthesised metallaboratranes containing a dative M → B bond (κ^3-*B*,*S*,*S*′ bonding) for second row transition metals of Groups 5, 9 and 10, and the third row metals Ta and Ir [12]. In the organometallic complexes mentioned above, the tridentate Tm or Bm acts as a capping ligand, very much like Cp or arene rings. Bailey [8a] reported the first synthesis of mixed sandwich complexes containing Tm and Cp or *p*-cymene, viz. $[(p\text{-cymene})Ru^{II}(Tm)]Cl$ (**A**) and $[CpRu^{II}\text{-}(Tm)]$ (**B**), from $[(p\text{-cymene})RuCl_2]_2$ and $[CpRu(MeCN)_3]^+$, respectively (Scheme 1). The latter reagent had been used in

* Corresponding author. Tel.: +65 68742677; fax:+65 67791691.
E-mail addresses: chmlwk@nus.edu.sg (W.K. Leong), chmgohly@nus.edu.sg (L.Y. Goh).

0022-328X/$ - see front matter © 2005 Published by Elsevier B.V.
doi:10.1016/j.jorganchem.2005.10.043

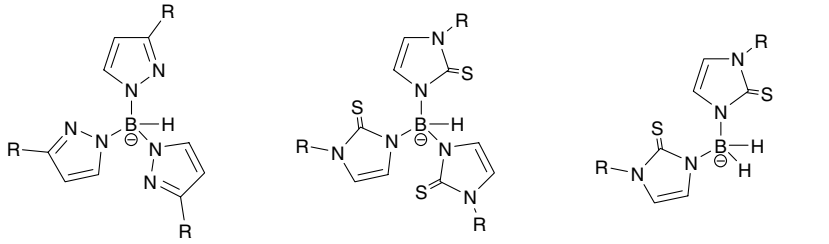

Chart 1.

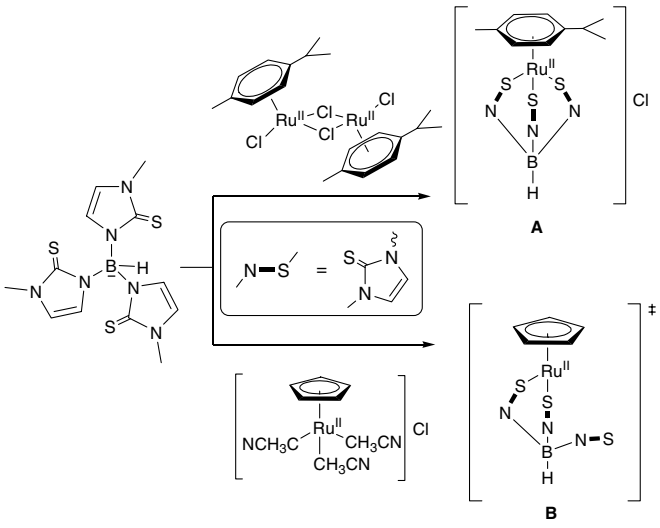

Scheme 1.

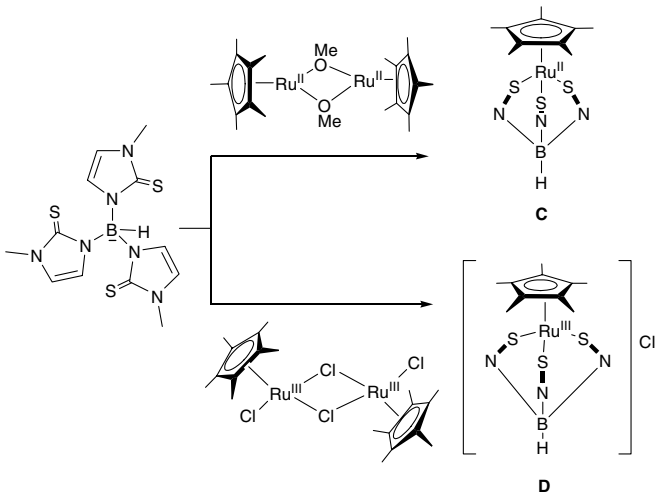

Scheme 2.

1986 by Mann [13] as the precursor to [CpRu^{II}(Tp)] which contains tridentate Tp. The splitting of Tm signals (1:2 relative intensity) found in the ^{1}H NMR spectrum of **B** in DMSO, was attributed to the presence of one 'dangling' (uncoordinated) and two coordinated *mt* rings of the Tm ligand, i.e., presumably bidentate coordination of Tm via two of its three S donor atoms [8a]. Meanwhile, Hill [12b] reported solid state structural evidence for κ^3-*H*, *S*, *S*′ coordination in (Tm)RuH(CO)(PPh$_3$), and Rabinovich [14] soon after observed evidence for the predominance of κ^3-*H*, *S*, *S*′ over κ^3-*S*, *S*′, *S*″ (for Tm) or κ^2-*S*, *S*′ (for Bm) in (dppe)Ni complexes. These reports are indicative of possible equilibria between κ^3-*S*, *S*′, *S*″ and κ^3-*H*, *S*, *S*′ coordination of Tm complexes in solution. We have since synthesised the allied complexes [Cp*Ru^{II}(Tm)] (**C**) and [Cp*Ru^{III}(Tm)]Cl (**D**) (Scheme 2) for such a study; indeed a combination of VT–^{1}H NMR spectral and cyclic voltammetric studies revealed that the tripodal Tm ligand underwent a facile κ^3-*S*, *S*′, *S*″ and κ^3-*H*, *S*, *S*′ coordination exchange depending on the oxidation state of Ru, resulting in an electrochemical square scheme mechanism [15]. (See discussions below). Since such electrochemical mechanisms are uncommon (or at least rarely detected), it is of interest to conduct comparative investigations on the effect of substitution of (i) the Cp* capping ligand with an arene ring and (ii) the Tm ligand with the Bm ligand in order to determine whether solution phase isomerizations are a common feature of (mercaptomethimazolyl)borate ligands coordinated to Ru.

This paper describes the syntheses, characterisation and electrochemistry of these Cp*/(HMB)Ru complexes containing Tm and Bm ligands.

2. Results and discussion

2.1. Synthetic studies

Using a synthetic methodology similar to that for [(*p*-cymene)Ru^{II}(Tm)]Cl (**A**) (Scheme 1) [8a], and [Cp*Ru^{III}-(Tm)]Cl (**D**) (Scheme 2) [15], [(HMB)Ru^{II}(Tm)]Cl (**1**) was obtained from the reaction of [(HMB)RuCl$_2$]$_2$ with KTm in 66% yield as a bright red crystalline solid (Scheme 3).

Likewise [(HMB)Ru(Bm)]Cl (**2**) was isolated as deep red crystals in 70% yield from an 8 h reaction of [(HMB)-RuCl$_2$]$_2$ with NaBm at room temperature (Scheme 4).

As in the reaction of [Cp*RuOMe]$_2$ with KTm to yield Cp*Ru^{II}(Tm) **C** [15], it was found that [Cp*RuOMe]$_2$ was a good precursor to Cp*Ru^{II}(Bm) (**3**), which was obtained as orange crystals in 85% yield from a 2 h reaction with NaBm at room temperature (Scheme 5).

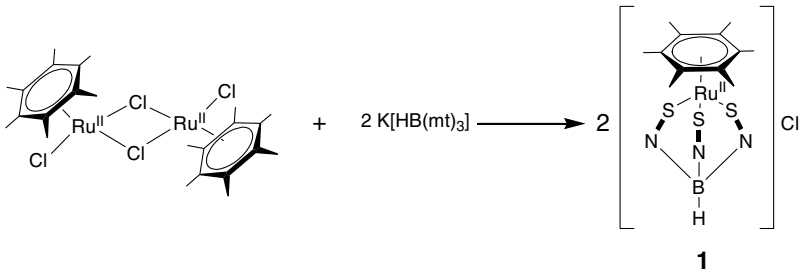

1

Scheme 3.

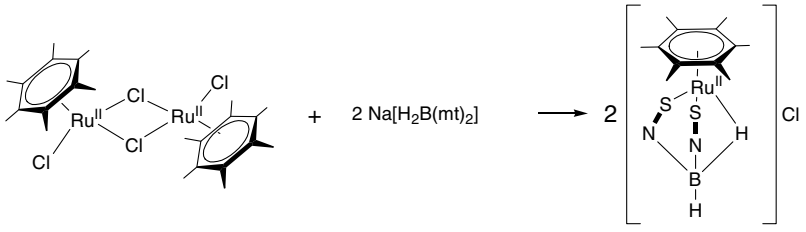

2

Scheme 4.

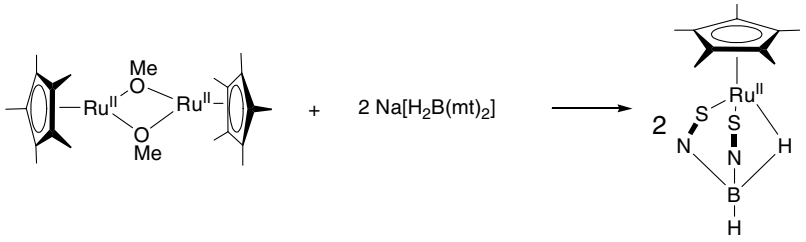

3

Scheme 5.

2.2. Proton NMR spectral characteristics

As in the case of **A**, the ^{1}H NMR spectrum of **1** is consistent with tridentate coordination of the Tm ligand. There was no sign of the solvent-dependent equilibrium observed in the solution of **C** between κ^3-*S*,*S*′,*S*″ (form I) and κ^3-*H*,*S*,*S*′ (form II) isomers, which were found to be present in relative concentration of 1:3 in a non-polar solvent like C_6D_6 and 0:1 in a polar solvent like CD_2Cl_2 (Scheme 6) [15].

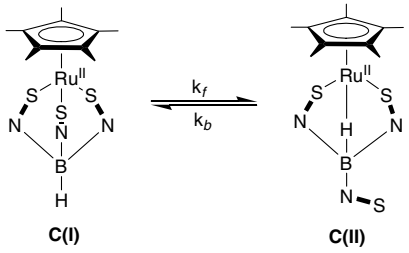

Scheme 6.

The ^{1}H NMR spectra of both **2** (in CD_3CN) and **3** (in C_6D_6) show a pair of doublets for the CH's of the imidazole rings in the region δ 5.75–6.96, and two very broad overlapping 'humps', due to unresolved boron quadrupolar coupling, centered at δ −10.84 for **2** and a quartet of equal intensity at δ −7.83 for **3**, for the agostic-like H's – consistent with κ^3-*H*,*S*,*S*′ coordination of the Bm ligand. In CD_2Cl_2 at 300 K, both these μ-HB resonances are observed as two very broad overlapping 'humps' (each possessing $\nu_{1/2}$ ca. 100 Hz), the resolution of which decreases further with lowering of temperature, until at 183 K, the 'humps' merged to give broad singlets ($\nu_{1/2}$ ca. 36, 50 Hz), presumably due to self-decoupling of the boron quadrupole at low temperatures. A similar observation was reported by Hill and coworkers [12b] for [(κ^3-*H*,*S*,*S*′-Tm)RuH(CO)(PPh_3)]. There was no sign of the occurrence of fluxional processes in **2** or **3**.

Despite evidence of their presence in their IR spectra, the B–H (terminal) protons of complexes **1**–**3** were not detected in their NMR spectra. In fact, such observations in complexes of Tm or Bm are rare, e.g. as very broad signals, δ 4.42–5.32 in (pzBm) complexes of Tl and Zn [5d], δ 3.57–3.75 in various $Bm^RMn(CO)_3$ complexes [8b]

and δ 4.63 ($v_{1/2}$ 160 Hz) in $PtMe_3(Tm)_3$ [12f]. In most complexes of Tm and Bm in the literature to date, the B–H (terminal) protons were not observed [4e,5b,5d,5i,6b,6c,8a,14], presumably on account of the broad nature of the multiplet caused by coupling to boron.

2.3. Crystallographic studies

The molecular structures of [(HMB)Ru(Tm)]Cl (**1**), [(HMB)Ru(Bm)]Cl (**2**) and [Cp*Ru(Bm)] (**3**) have been determined by single crystal X-ray diffraction analysis. The compounds crystallize in trigonal $P\bar{3}$, monoclinic $C2/m$ and monoclinic $C2/c$ space groups, respectively. The unit cells of **2** and **3** contain solvent molecules, 0.25 CH_2Cl_2 and 0.25 toluene, respectively.

The molecular structures of the three compounds, depicted in Figs. 1–3, are markedly similar, each containing a ruthenium center sandwiched between either an arene or a Cp* ligand and a tripodal ligand, κ^3-S,S',S'' (Tm) or κ^3-H,S,S' (Bm). The latter coordination mode via two thione sulphurs and one agostic-like hydrogen has been found to be a recurrent feature in many Bm complexes, e.g., $[BmLi]_2$, $[BmTl]_x$ and BmZnX (X = I, Me and NO_3) [3], $(Bm^R)_2M$ (M = Zn, Cd and Hg [5i] and U [16]), $(Bm^R)M(CO)_3$ (M = Tc [11a] and Re [11a,11b,11c] and Mn [8b]) and [(Bm)Ni(dppe)]Cl [14].

The structure of **1** cation possesses a threefold axis of symmetry brought about by disorder in the Tm ligand; this axis passes through the centroid of the HMB ring, Ru(1) and B(1). In the structure of the Bm-containing complex **2**, a plane of symmetry cuts through the arene ring, Ru(1), B(1) and both H atoms. The B–H hydrogen atoms of the ligands were located and refined; the B–$H_{terminal}$ distances

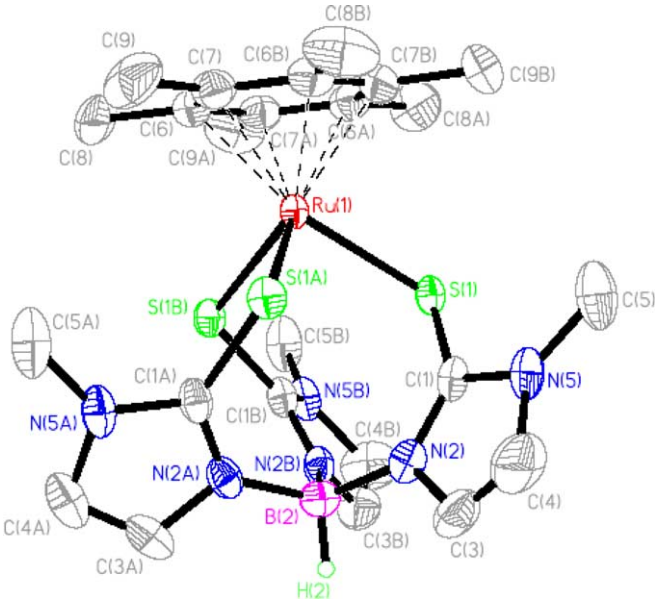

Fig. 1. Ortep plot of monocation of **1** (selected view which omits the disorder in the Tm ligand, H atoms on HMB and Tm are omitted for clarity). Thermal ellipsoids are drawn at the 50% probability level.

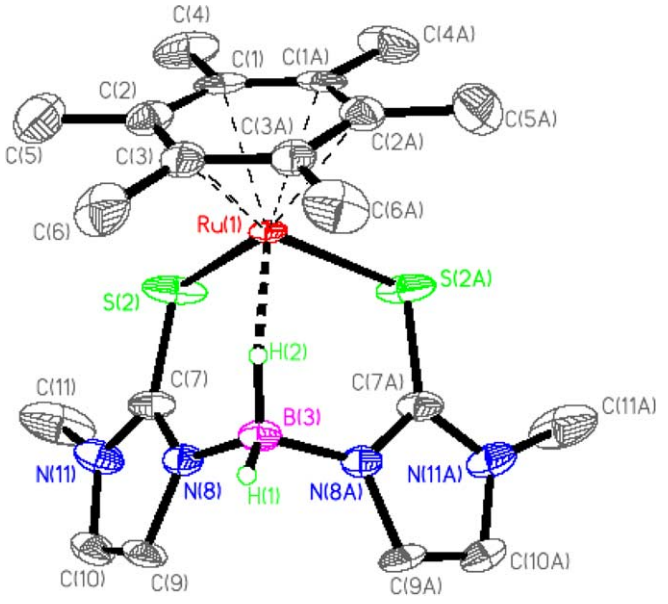

Fig. 2. Ortep plot of monocation of **2** (H atoms on HMB and Bm are omitted for clarity). Thermal ellipsoids are drawn at the 50% probability level.

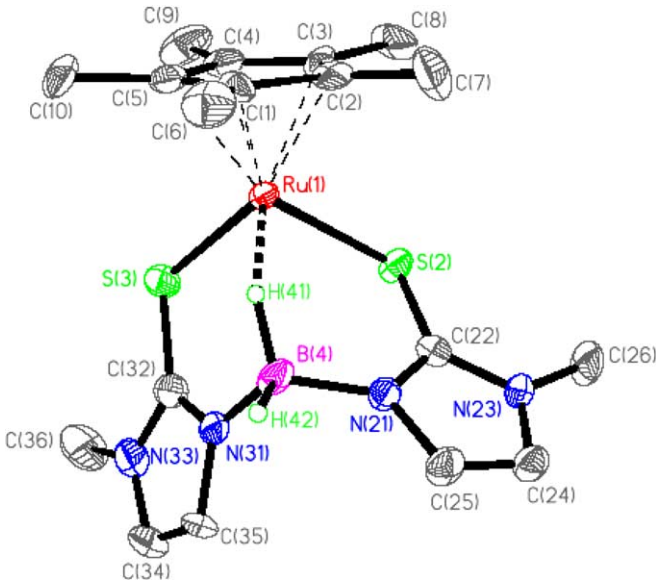

Fig. 3. Ortep plot of **3** (H atoms on Cp* and Bm are omitted for clarity). Thermal ellipsoids are drawn at the 50% probability level.

were 1.01(2), 0.96(2) and 1.18(1) Å for **1**, **2** and **3**, respectively. The B–$H_{agostic}$ bond distances were 1.08(2) and 1.17(1) Å in **2** and **3**, respectively; with corresponding Ru–$H_{agostic}$–B angles of 151(1)° and 140(1)°. These bond parameters compare with corresponding values of 1.29(5) Å and 137(4)° in [RuH(CO)(PPh_3)(κ^3-H,S',S'(Tm))] [12b]. The agostically connected Ru...H distances in **2** and **3** are 1.81(2) and 1.81(1) Å, respectively, with corresponding $H_{terminal}$–B–$H_{agostic}$ angles of 112(1)° and 110(1)°. The Ru–S distances in **1** fall within the range found in complexes (**A**) (range 2.3931(7)–2.4222(7) Å) [8a], and (**D**) (range

2.3213(8)–2.4100(8) Å) [15]. The Ru–S lengths in **3** are closer to those of the Tm complexes **1** and **A** than those in the Bm complex **2**. While the longer Ru–S bond lengths are close to those observed by Hill and coworkers for [RuH(CO)(PPh_3){κ^3-*H*,*S*,*S*′-HB(mt)$_3$}] and the ruthenaboratrane complex [range 2.4066(14)–2.4857(14) Å] [12a], the shorter ones resemble closely those (range 2.3396(10)–2.3851(10) Å) found in [(HMB)Ru^{II}(9S3)] [17a] and [Cp*Ru^{III}(9S3)]PF_6 [17b], in which 9S3 (trithiacyclononane) functions as a tripodal S_3 ligand like Tm. The Ru–(HMB)/Cp* (centroid) distances in **1**, **2** and **3** are very similar. The C–S bonds of the molecules fall in the range of 1.698(9)–1.786(12) Å, intermediate between values of a single bond (ca. 1.81 Å) and a double bond (ca. 1.56 Å), [18] as commonly found in metal complexes of Tm^R. The S–Ru–S angles in **1**, **2** and **3** are close to similar bite angles in complexes **A** [8a], **C** and **D** [15], and ruthenaboratrane [12a]. They are generally larger than those that we have found for 9S3 complexes of (HMB)Ru(II) [17a] and Cp*Ru(III) [17b] (range 85.18(4)–92.18(4)°). This difference can be attributed to the steric bulk of the imidazole rings in Tm and Bm ligands and/or higher flexibility of these ligands, compared with that of the ethylene bridges in 9S3 (see Table 1).

2.4. Cyclic voltammetry

Cyclic voltammograms obtained at a GC electrode in 0.5 mM solutions of **1**–**3** in CH_2Cl_2 at 233 K (—) and 293 K (···) are shown in Fig. 4. **3** displayed a one-electron oxidation process with a reversible half-wave potential

Table 1
Selected bond lengths (Å) and bond angles (°) for **1**, **2** and **3**

1			
Ru(1)–S(1)	2.4024(15)	C(1)–S(1)[a]	1.772(13)
			1.786(12)
			1.786(12)
B(2)–H(2)	1.01(2)	Ru–(HMB)centroid	1.70(1)
S(1)–Ru(1)–(S1A)	91.06(5)	Ru(1)–S(1)–C(1)[a]	108.1(4)
			107.8(4)
			107.8(4)
2			
Ru(1)–S(2)	2.376(3)	Ru(1)...H(2)	1.81(2)
B(3)–H(1)	0.96(2)	C(7)–S(2)	1.703(8)
B(3)–H(2)	1.08(2)	Ru–(HMB)centroid	1.70(1)
S(2)–Ru(1)–(S2A)	90.09(16)	H(1)–B(3)–H(2)	112(1)
Ru(1)–S(2)–C(7)	105.7(3)	Ru(1)...H(2)–B(3)	151(1)
3			
Ru(1)–S(2)	2.416(2)	Ru(1)...H(2)	1.81(2)
Ru(1)–S(3)	2.392(2)	C(22)–S(2)	1.701(9)
B(4)–H(42)	1.18(1)	C(32)–S(3)	1.698(9)
B(4)–H(41)	1.17(1)	Ru–(HMB)centroid	1.77(1)
S(2)–Ru(1)–(S3)	93.22(8)	H(1)–B(3)–H(2)	110(1)
Ru(1)–S(2)–C(22)	104.5(3)	Ru(1)...H(2)–B(3)	140(1)
Ru(1)–S(3)–C(32)	104.7(3)		

[a] Refer to disorder modelling described in the experimental.

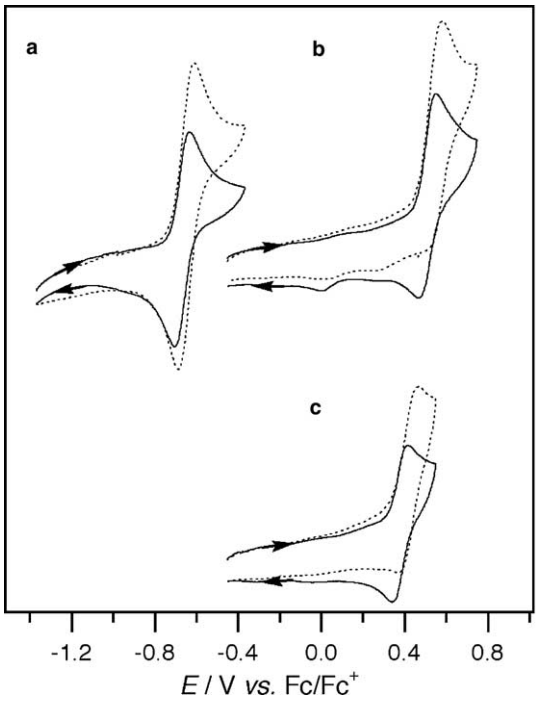

Fig. 4. Cyclic voltammograms performed at a 1 mm diameter planar GC electrode in CH_2Cl_2 (0.25 M Bu_4NPF_6) at (—) 233 K or (···) 293 K and a scan rate of 100 mV s^{-1} for 0.5 mM (a) **3**, (b) **2** and (c) **1**.

($E^r_{1/2}$) of −0.670 V vs. Fc/Fc^+. The $E^r_{1/2}$-value [that approximates the formal potential (E^0)] was calculated from CV data under conditions where the ratio of the oxidative (i^{ox}_p) to reductive (i^{red}_p) peak currents were equal to unity and using the relationship

$$E^r_{1/2} = (E^{ox}_p + E^{red}_p)/2, \quad (1)$$

where E^{ox}_p and E^{red}_p are the anodic and cathodic peak potentials respectively. The $E^r_{1/2}$-value for **3** was close to that observed for similar Cp*Ru^{II} compounds containing the [HB(mt)$_3$] ligand, such as κ^3-*S*,*S*′,*S*″-[Cp*Ru^{II}{HB(mt)$_3$}] and κ^3-*H*,*S*,*S*′-[Cp*Ru^{II}{HB(mt)$_3$}] that were oxidized by one electron at $E^r_{1/2} = -0.86$ and -0.65 V vs. Fc/Fc^+, respectively [15].

For both **1** and **2**, the anodic (i^{ox}_p) to cathodic (i^{red}_p) ratios (i^{ox}_p/i^{red}_p) measured by cyclic voltammetry were significantly >1 over all measured temperatures at a scan rate of 0.1 V s^{-1}, indicating that the oxidized Ru^{III} compounds were relatively unstable, especially at higher temperatures (Fig. 4(b) and (c)). This is in contrast to the higher stability observed for **3** (Fig. 4(a)), which has i^{ox}_p/i^{red}_p-values close to 1 over all temperatures measured (Fig. 4(a)). The $E^r_{1/2}$ values for **1** and **2** were obtained from the peak potentials measured by square wave voltammetry and were +0.42 and +0.56 V vs. Fc/Fc^+ respectively. It is apparent from the cyclic voltammograms in Fig. 4 that the $E^r_{1/2}$-values are very sensitive to the Cp* and HMB ligands (compare Figs. 4(a) and (b)), and less sensitive to the difference in the [H_2B(mt)$_2$] and [HB(mt)$_3$] ligands (compare Figs. 4(b) and (c)). The ~1 V difference between the $E^r_{1/2}$ values of

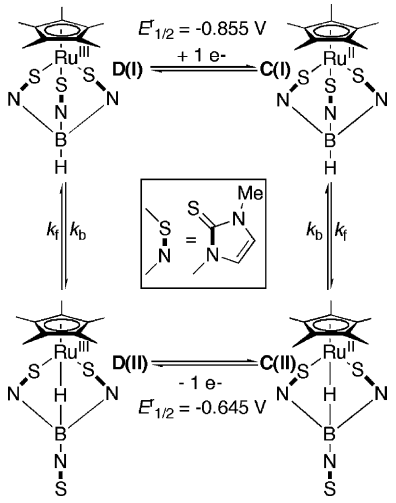

Scheme 7. Square scheme mechanism (modified from reference [15]).

the Cp* and HMB coordinated compounds may be due to the positive charge on the $[(HMB)Ru^{II}\{H_2B(mt)_2\}]^+$ and $[(HMB)Ru^{II}\{HB(mt)_3\}]^+$ complexes, which makes the removal of an electron more difficult than from the neutral $[(Cp^*)Ru^{II}\{H_2B(mt)_2\}]$ and $[(Cp^*)Ru^{II}\{HB(mt)_3\}]$ [15] complexes.

Recent work from these laboratories demonstrated that the $[(Cp^*)Ru^{II/III}\{HB(mt)_3\}]$ complexes underwent an isomerization reaction involving κ^3-*H*, *S*, *S*′-and κ^3-*S*, *S*′, *S*″-coordination of the $[HB(mt)_3]$ ligand [15]. Because both the reduced and oxidized ruthenium compounds underwent the chemically reversible structural change, a ''square scheme'' mechanism resulted, enabling cyclic voltammetry to be used to determine the rate constants for the homogeneous isomerizations that occurred following electron transfer (Scheme 7). However, cyclic voltammetry experiments performed on **1**, the HMB analogue of $[(Cp^*)Ru^{II}\{HB(mt)_3\}]$, did not provide supporting evidence for the occurrence of an isomerization reaction involving κ^3-*H*, *S*, *S*′-and κ^3-*S*, *S*′, *S*″-coordination of the $[HB(mt)_3]$ ligand in HMB coordinated complexes. One reason for the failure to detect an isomerization reaction (should it actually occur) may be due to the inherent instability of $[(arene)Ru^{III}]$ complexes [19], which could result in the oxidized compound ($\mathbf{1}^{2+}$) simply decomposing at a rate faster than the rate of rearrangement of the $[HB(mt)_3]$ ligand. Cyclic voltammetry experiments performed on the compounds containing the S_2 ligand $[H_2B(mt)_2]$ (Figs. 4(a) and (b)) also did not lead to any obvious signs of an isomerization reaction following electron transfer in either the Cp*- or HMB-containing complexes.

3. Conclusions

Monocationic (HMB)Ru(II) complexes of Tm and Bm have been synthesised from the reactions of $[(HMB)RuCl_2]_2$ with KTm and NaBm, respectively, and a neutral Cp*Ru(II) complex of Bm from the reaction of $[Cp^*RuOMe]_2$ with NaBm. Single crystal X-ray analysis shows tripodal coordination of both Tm (κ^3-*S*, *S*′, *S*″) and Bm (κ^3-*H*, *S*, *S*′) in the solid state complexes. Cyclic voltammetric measurements indicated that the (HMB)Ru(II) complexes (**1** and **2**) were substantially harder to oxidize than their (Cp*)Ru(II) analogue (**3**), and the (HMB)Ru(III) complexes of Tm and Bm were less chemically stable than the (Cp*)Ru(III) complexes of Tm and Bm. Surprisingly, no evidence (electrochemical or NMR spectroscopic) was found for the existence of a κ^3-*S*, *S*′, *S*″ and κ^3-*H*, *S*, *S*′ equilibrium in the $[(HMB)Ru^{II/III}(Tm)]$ complexes, which was previously found to occur in the Cp* containing analogues [15]. Therefore, the solution phase chemistry of the Tm anion coordinated to closely related metal systems (such as Cp*Ru and (HMB)Ru) can not be assumed and must be ascertained individually, preferably by correlating a range of analytical techniques.

4. Experimental

4.1. General procedures

All reactions were carried out using conventional Schlenk techniques under an inert atmosphere of nitrogen or under argon in an M. Braun Labmaster 130 Inert Gas System. NMR spectra were measured on a Bruker 300 MHz FT NMR spectrometer; ^1H and ^{13}C chemical shifts were referenced to residual C_6H_6 in C_6D_6, tetramethylsilane in CD_2Cl_2 or CH_2DCN in CD_3CN. IR spectra were measured in the range of 4000–600 cm^{-1} by means of a Shimadzu IRPrestige-21 FTIR instrument. Mass spectra were run on Finnigan Mat 95XL-T and Mat LCQ spectrometers. Cyclic voltammetric experiments were conducted with a 1 mm diameter glassy carbon working electrode and a computer controlled Eco Chemie μ Autolab III potentiostat. The electrochemical cell was jacketed in a glass sleeve and cooled between 233 and 293 K using a Lauda RL6 variable temperature methanol-circulating bath. Elemental analyses were carried out by the microanalytical laboratory in-house. Potassium hyrdotris(methimazolyl)borate (KTm, where $Tm = [HB(mt)_3]$, i.e., $[(C_4H_5N_2S)_3BH]$) [20], sodium hydrobis(methimazolyl)borate(NaBm, where $Bm = [H_2B(mt)_2]$, i.e., $[(C_4H_5N_2S)_2BH_2]$) [5i] $[(HMB)RuCl_2]_2$ and Cp*RuOMe ($Cp^* = C_5Me_5$) were synthesized as reported in the literature [21,22]. 2-Mercapto-1-methimazolyl was used as purchased from Lancaster Synthesis Ltd and $RuCl_3 \cdot 3H_2O$ was used as purchased from Pressure Chemical Co. Solvents were dried over sodium benzophenone or calcium hydride and distilled before use. Celite (Fluka AG) was dried at 140 °C overnight before use.

4.2. Reactions of $[(HMB)RuCl_2]_2$

(a) *With KTm.* To an orange-red suspension of $[(HMB)RuCl_2]_2$ (33 mg, 0.05 mmol) in CH_2Cl_2 was added $K[HB(mt)_3]$ (39 mg, 0.10 mmol). The mixture was stirred for 10 h, resulting in a suspension of a white precipitate of KCl in a deep red supernatant. The suspension was

filtered and the red filtrate was evacuated to dryness and recrystallised in MeOH/ether at −30 °C. An air stable, bright red crystalline solid of [(HMB)Ru(Tm)]Cl (**1**) (43 mg, 0.07 mmol, 66% yield) was obtained after a day. Anal. Found: C, 43.2; H, 5.4; N, 12.9; S, 14.7%. Calc. for $C_{24}H_{34}BClN_6RuS_3 \cdot 0.7H_2O$: C, 43.5; H, 5.4; N, 12.7; S, 14.5%. IR (CH_2Cl_2, cm^{-1}): ν(B–H) 2440w. FAB$^+$-MS: *m/z* 615 [M^+, $C_6Me_6Ru(C_4H_5N_2S)_3BH$]; 501 [$M^+ - (C_4H_5N_2S)H$]; 452 [$M^+ - (C_6Me_6)H$]; 377 [$M^+ - (C_4H_5N_2S)_2BH$]; 339 [$M^+ - (C_6Me_6)(C_4H_5N_2S)H$]. HR-FAB$^+$-MS: *m/z* for [$M^+$] 615.1164 (found), 615.1137 (calc.). ^{1}H NMR (δ, CD_3CN): 7.03 (d, $3 \times 1H$, $^3J = 1.7$ Hz, CH imidazole), 6.86 (d, $3 \times 1H$, $^3J = 1.7$ Hz, CH imidazole), 3.63 (s, $3 \times 3H$, N-CH_3), 2.15 (s, H_2O, relative proportion of H_2O:**1** = ca. 0.5, from peak integrals), 2.05 (s, 18H, $C_6(CH_3)_6$). ^{13}C NMR (δ, CD_3CN): 157.8 (s, S*C*N_2HC═CH), 124.7 (s, C imidazole), 121.8 (s, C imidazole), 95.5 (s, $C_6(CH_3)_6$), 35.7 (s, N-*C*H_3) 15.5 (s, $C_5(CH_3)_5$).

(b) *With NaBm*. To orange-red solution of [(HMB)-$RuCl_2]_2$ (67 mg, 0.10 mmol) in THF was added NaBm (54 mg, 0.20 mmol) and the mixture was stirred for 8 h, giving a red suspension. The suspension was filtered to give a red residue and a light red solution, from which ca. 5 mg of unreacted [(HMB)$RuCl_2]_2$ was recovered. The red solid was extracted with CH_2Cl_2 (5×2 mL). The red extract was concentrated to ca. 3 mL and ca. 2 mL of hexane added. Deep red, air stable crystals of [(HMB)Ru(Bm)]Cl (**2**) (75 mg, 0.14 mmol, 70% yield) were obtained after 2 days at −30 °C. Anal. Found: C, 44.2; H, 5.5; N, 10.3; S, 12.0%. Calc. for $C_{20}H_{30}BClN_4RuS_2$: C, 44.7; H, 5.6; N, 10.4; S, 11.9%. IR (KBr, cm-1): ν(B–H) 2438w; ν(μ-B–H) 2162w, 2047w. FAB$^+$-MS: *m/z* 503 [M^+, $C_6Me_6Ru(C_4H_5N_2S)_2BH_2$]; 377 [$M^+ - (C_4H_5N_2S)BH_2$], 339 [$M^+ - (C_6Me_6)H_2$]. ^{1}H NMR ($\delta$,$CD_3CN$): 6.96 (d, $2 \times 1H$, $^3J = 2.5$ Hz, CH imidazole), 6.78 (d, $2 \times 1H$, $^3J = 2.5$ Hz, CH imidazole), 3.53 (s, $2 \times 3H$, N-CH_3), 2.14 (s, 18H, $C_6(CH_3)_6$), −10.84 (center of two overlapping 'humps' at δ −10.70 ($\nu_{1/2}$ ca. 90 Hz) and δ −10.97 ($\nu_{1/2}$ ca. 110 Hz), 1H, μ-HB). ^{13}C NMR (δ, CD_3CN): 163.1 (s, S*C*N_2HC═CH), 124.3 (s, C imidazole), 121.6 (s, C imidazole), 97.2 (s, $C_6(CH_3)_6$), 34.9 (s, N-*C*H_3) 16.2 (s, $C_5(CH_3)_5$). ^{1}H NMR (δ, CD_2Cl_2, μ-HB): 300 K: −10.94 center of two overlapping 'humps' at δ −10.83 ($\nu_{1/2}$ ca. 97 Hz) and δ −11.05 ($\nu_{1/2}$ ca. 102 Hz); 183 K: −10.93 ($\nu_{1/2}$ ca. 36 Hz).

4.3. Reaction of [Cp*Ru(OMe)]$_2$ with NaBm

To a dark pink solution of [Cp*Ru(OMe)]$_2$ (52 mg, 0.10 mmol) in toluene was added NaBm (54 mg, 0.20 mmol) and the suspension stirred for 2 h. The resultant suspension of a white precipitate of KOMe in a bright orange solution was then filtered through a thin disc of Celite on a glass sinter.

Table 2
Data collection and processing parameters

Complexes	**1**	**2**(0.25CH_2Cl_2)	**3**(0.25C_7H_8)
Formula	$C_{24}H_{34}BClN_6RuS_3$	$C_{20.50}H_{31}BCl_2N_4RuS_2$	$C_{19.75}H_{29}BN_4RuS_2$
M_r	650.08	580.39	498.47
Temperature (K)	223(2)	223(2)	223(2)
Crystal color and habit	Red, block	Red, needle	Red, plate
Crystal size (mm)	$0.34 \times 0.30 \times 0.14$	$0.40 \times 0.11 \times 0.09$	$0.14 \times 0.12 \times 0.02$
Crystal system	Trigonal	Monoclinic	Monoclinic
Space group	$P\bar{3}$	$C2/m$	$C2/c$
a (Å)	13.2095(7)	19.637(7)	14.2301(7)
b (Å)	13.2095(7)	1411.703(4)	14.2921(7)
c (Å)	9.9220(11)	11.970(4)	24.8174(12)
α (°)	90	90	90
β (°)	90	105.109(7)	106.524 (2)
γ (°)	120	90	90
V (Å^3)	1499.3(2)	2655.6(17)	4838.9(4)
Z	2	4	8
Density (Mg m^{-3})	1.440	1.452	1.368
Absorption coefficient (mm^{-1})	0.845	0.964	0.832
F(000)	668	1188	2052
Θ range for data collection	2.05–26.37	2.05–29.83	2.06–26.37
Index ranges	$-16 \leqslant h \leqslant 8$, $0 \leqslant k \leqslant 16$, $0 \leqslant l \leqslant 12$	$-26 \leqslant h \leqslant 25$, $0 \leqslant k \leqslant 16$, $0 \leqslant l \leqslant 16$	$-17 \leqslant h \leqslant 17$, $0 \leqslant k \leqslant 17$, $0 \leqslant l \leqslant 30$
No. of reflections collected	11422	15089	34190
Independent reflections [R(int)]	2065 [0.0516]	3684 [0.0828]	4959 [0.1126]
No. of data/restraints/parameters	2056/0/161	3684/1/177	4959/2/260
Final R indices [$I > 2\sigma(I)$][a,b]	$R_1 = 0.0679$, $wR_2 = 0.1898$	$R_1 = 0.1092$, $wR_2 = 0.2553$	$R_1 = 0.1025$, $wR_2 = 0.2128$
R indices (all data)	$R_1 = 0.0778$, $wR_2 = 0.1992$	$R_1 = 0.1175$, $wR_2 = 0.2603$	$R_1 = 0.1136$, $wR_2 = 0.2187$
Goodness-of-fit on F^2[c]	1.178	1.281	1.318
Large diff. peak and hole (e Å^{-3})	3.859 and −0.868	2.584 and −1.983	1.487 and −1.988

[a] $R = (\sum|F_o| - |F_c|)\sum|F_o|$.
[b] $wR_2 = [(\sum\omega|F_o| - |F_c|)^2/\sum\omega|F_o|^2]^{1/2}$.
[c] GoF $= [(\sum\omega|F_o| - |F_c|)^2/(N_{obs} - N_{param})]^{1/2}$.

The orange filtrate was evacuated to dryness and recrystallised in THF/hex at −30 °C. An air stable bright orange crystalline solid of Cp*Ru(Bm) (**3**) (81 mg, 0.17 mmol, 85% yield) was obtained after 2 days. Anal. Found: C, 45.3; H, 5.5; N, 11.6; S, 13.4%. Calc. for $C_{18}H_{27}BN_4RuS_2$: C, 45.5; H, 5.7; N, 11.8; S, 13.5%. IR (KBr, cm^{-1}): ν(B–H) 2422w; ν(μ-B–H) 2073w. ESI$^+$-MS: m/z 476 [M^+, $C_5Me_5Ru(C_4H_5N_2S)_2BH_2$]. ^{1}H NMR ($\delta$, C_6D_6): 6.41 (d, 2×1H, $^3J = 1.7$ Hz, CH imidazole), 5.75 (d, 2×1H, $^3J = 1.7$ Hz, CH imidazole), 2.83 (s, 2×3H, N-CH_3), 1.92 (s, 15H, Cp-CH_3), −7.83 (q of equal intensity, 1H, $J_{BH} = 65$ Hz, μ-HB). ^{13}C NMR (δ, C_6D_6): 169.4 (s, S*C*N_2HC=CH), 120.6 (s, C imidazole), 120.4 (s, C imidazole), 79.1 (s, *C*$_5$(CH$_3$)$_5$), 34.4 (s, N-*C*H$_3$) 11.6 (s, C$_5$(*C*H$_3$)$_5$). ^{1}H NMR (δ, CD_2Cl_2, μ-HB): 300 K: −8.51 center of two overlapping 'humps' at δ −8.37 ($\nu_{1/2}$ ca. 100 Hz) and δ −8.65 ($\nu_{1/2}$ ca. 125 Hz); 183 K: −8.90 br ($\nu_{1/2}$ ca. 50 Hz).

4.4. X-ray structure determinations

Diffraction-quality single crystals were obtained at −30 °C as follows: **1** as red blocks by slow diffusion of ether into a methanol solution after 7 days; **2** as red needles by slow diffusion of ether into a dichloromethane solution after 5 days and **3** as red plates from THF–hexane solutions, after 3 days. The crystals were mounted on glass fibres. X-ray data were collected on a Bruker APEX AXS diffractometer, equipped with a CCD detector, using Mo Kα radiation (λ 0.71073 Å). The program SMART [23] was used for collecting frames of data, indexing reflection and determination of lattice parameter, SAINT [23] for integration of the intensity of reflections, scaling, and for correction of Lorentz and polarization effects, SADABS [24] for absorption correction, and SHELXTL [25] for space group and structure determination, and least-squares refinements on F^2. The structures for **1**, **2** and **3** were solved by direct methods to locate the heavy atoms, followed by difference maps for the light non-hydrogen atoms. The B–H hydrogen atoms were located and refined; all other hydrogen atoms were in calculated positions. There was disorder of the scorpionate ligand in **1**. This was modeled with two alternative positions of equal occupancies for the imidazole rings in which the C=C portions were coincident. The hydrogen atoms were placed and refined in a riding model. There was also disorder in the Cl^- counterion, which was modeled with two alternative sites and the occupancies summed to unity. The crystal data collection and processing parameters are given in Table 2.

5. Supporting information available

Crystallographic data for the structural analysis has been deposited with the Cambridge Crystallographic Data Centre, CCDC Nos. 269688–269690 for compounds **1**, **2** and **3** respectively. Copies of this information may be obtained free of charge from The Director, CCDC, 12 Union Road, Cambridge, CB2 1EZ, UK (fax: +44 1223 336033; email: deposit@ccdc.cam.ac.uk or www:http://www.ccdc.cam.ac.uk).

Acknowledgement

Support from the National University of Singapore for Academic Research Grant No. R143-000-209-112 (to L.Y.G.) is gratefully acknowledged.

References

[1] (a) M. Garner, J. Reglinski, I.D. Cassidy, M.D. Spicer, A.R. Kennedy, Chem. Commun. (1996) 1975;
(b) J. Reglinski, M. Garner, I.D. Cassidy, P.A. Slavin, M.D. Spicer, D.R. Armstrong, J. Chem. Soc., Dalton Trans. (1999) 2119.
[2] (a) S. Trofimenko, Scorpionates: The Coordination Chemistry of Polypyrazolylborate Ligands, Imperial College Press, London, 1999, and references therein;
(b) S. Trofimenko, Polyhedron 23 (2004) 197;
(c) C. Pettinari, C. Santini, Comp. Coord. Chem. II 1 (2003) 159.
[3] C. Kimblin, B.M. Bridgewater, T. Hascall, G. Parkin, J. Chem. Soc., Dalton Trans. (2000) 891.
[4] (a) C. Santini, G. Lobbia, C. Pettinari, M. Pellei, G. Valle, S. Calogero, Inorg. Chem. 37 (1998) 890;
(b) C. Santini, C. Pettinari, G. Lobbia, R. Spagna, M. Pellei, F. Vallorani, Inorg. Chim. Acta 285 (1999) 81;
(c) J.F. Ojo, P.A. Slavin, J. Reglinski, M.D. Spicer, M. Garner, A.R. Kennedy, S.J. Teat, Inorg. Chim. Acta 313 (2001) 15;
(d) B.M. Bridgewater, G. Parkin, J. Am. Chem. Soc. 122 (2000) 7140;
(e) M. Garner, M. Lehmann, J. Reglinski, M.D. Spicer, Organometallics 20 (2001) 5233;
(f) M. Tesmer, M. Shu, H. Vahrenkamp, Inorg. Chem. 40 (2001) 4022;
(g) D.V. Patel, D.J. Milhalcik, K.A. Kreisel, G.P.A. Yap, L.N. Zakharov, W.S. Kassel, A.L. Rheingold, D. Rabinovich, J. Chem. Soc., Dalton Trans. (2005) 2410.
[5] (a) M. Garner, K. Lewinski, A. Pattek-Janczyk, J. Reglinski, B. Sieklucka, M.D. Spicer, M. Szaleniec, J. Chem. Soc., Dalton Trans. (2003) 1181;
(b) D.J. Mihalcik, J.L. White, J.M. Tanski, L.N. Zakharov, G.P.A. Yap, C.D. Incarvito, A.L. Rheingold, D. Rabinovich, J. Chem. Soc., Dalton Trans. (2004) 1626;
(c) C.A. Dodds, M.-A. Lehmann, J.F. Ojo, J. Reglinski, M.D. Spicer, Inorg. Chem. 43 (2004) 4927;
(d) C. Kimblin, B.M. Bridgewater, T. Hascall, G. Parkin, J. Chem. Soc., Dalton Trans. (2000) 1267;
(e) P.A. Slavin, J. Reglinski, M.D. Spicer, A.R. Kennedy, J. Chem. Soc., Dalton Trans. (2000) 239;
(f) C.A. Dodds, M. Jagoda, J. Reglinski, M.D. Spicer, Polyhedron 23 (2004) 445;
(g) B.M. Bridgewater, G. Parkin, Inorg. Chem. Commun. 3 (2000) 534;
(h) C.A. Dodds, A.R. Kennedy, J. Reglinski, M.D. Spicer, Inorg. Chem. 43 (2004) 394;
(i) H.M. Alvarez, T.B. Tran, M.A. Richter, D.M. Alyounes, D. Rabinovich, J.M. Tanski, M. Krawiec, Inorg. Chem. 42 (2003) 2149.
[6] (a) I. Cassidy, M. Garner, A.R. Kennedy, G.B.S. Potts, J. Reglinski, P.A. Slavin, M.D. Spicer, Eur. J. Inorg. Chem. (2002) 1235;
(b) S. Bakbak, V.K. Bhatia, C.D. Incarvito, A.L. Rheingold, D. Rabinovich, Polyhedron 20 (2001) 3343;
(c) J.L. White, J.M. Tanski, D. Rabinovich, J. Chem. Soc., Dalton Trans. (2002) 2987.
[7] C. Santini, M. Pellei, G.G. Lobbia, C. Pettinari, A. Drozdov, S. Troyanov, Inorg. Chim. Acta 325 (2001) 20.
[8] (a) P.J. Bailey, D.J. Lorono-Gonzales, C. McCormack, S. Parsons, M. Price, Inorg. Chim. Acta 354 (2003) 61;

(b) L.A. Graham, A.R. Fout, K.R. Kuehne, J.L. White, B. Mookherji, F.M. Marks, G.P.A. Yap, L.N. Zakharov, A.L. Rheingold, D. Rabinovich, J. Chem. Soc., Dalton Trans. (2005) 171.
[9] M.R.St.-J. Foreman, A.F. Hill, A.J.P. White, D.J. Williams, Organometallics 22 (2003) 5593.
[10] M.R.St.-J. Foreman, A.F. Hill, N. Tshabang, A.J.P. White, D.J. Williams, Organometallics 22 (2003) 3831.
[11] (a) R. Garcia, A. Paulo, A. Domingos, I. Santos, K. Ortner, R. Alberto, J. Am. Chem. Soc. 122 (2000) 11240;
(b) R. Garcia, A. Paulo, A. Domingos, I. Santos, J. Organomet. Chem. 632 (2001) 41;
(c) R. Garcia, A. Paulo, A. Domingos, I. Santos, R. Alberto, Inorg. Chem. 41 (2002) 2422;
(d) R. Garcia, A. Paulo, A. Domingos, I. Santos, J. Chem. Soc., Dalton Trans. (2003) 2757.
[12] (a) A.F. Hill, G.R. Owen, A.J.P. White, D.J. Williams, Angew. Chem. Int. Ed. 38 (1999) 2759;
(b) M.R.St.-J. Foreman, A.F. Hill, G.R. Owen, A.J.P. White, D.J. Williams, Organometallics 22 (2003) 4446;
(c) I.R. Crossley, A.F. Hill, A.C. Willis, Organometallics 24 (2005) 1062;
(d) I.R. Crossley, A.F. Hill, E.R. Humphrey, A.C. Willis, Organometallics 24 (2005) 4083;
(e) A.F. Hill, M.K. Smith, Chem. Commun. (2005) 1920;
(f) I.R. Crossley, A.F. Hill, A.C. Willis, Organometallics 24 (2005) 4889.
[13] A.M. McNair, D.C. Boyd, K.R. Mann, Organometallics 5 (1986) 303.
[14] H.M. Alvarez, J.M. Tanski, D. Rabinovich, Polyhedron 23 (2004) 395.
[15] S.L. Kuan, W.K. Leong, L.Y. Goh, R.D. Webster, Organometallics 24 (2005) 4639.
[16] L. Maria, Â. Domingos, I. Santos, Inorg. Chem. 40 (2001) 6863.
[17] (a) R.Y.C. Shin, M.A. Bennett, L.Y. Goh, W. Chen, D.C.R. Hockless, W.K. Leong, K. Mashima, A.C. Willis, Inorg. Chem. 42 (2003) 96;
(b) L.Y. Goh, M.E. Teo, S.B. Khoo, W.K. Leong, J.J. Vittal, J. Organomet. Chem. 664 (2002) 161.
[18] L. Pauling, in: The Nature of The Chemical Bond, third ed., Cornell University Press, Oxford, 1960, p. 268 and 274 (Chapter 8).
[19] R.Y.C. Shin, S.Y. Ng, G.K. Tan, L.L. Koh, S.B. Khoo, L.Y. Goh, R.D. Webster, Organometallics 23 (2004) 547.
[20] L.F. Soares, R.M. Silva, Inorg. Synth. 33 (2002) 199.
[21] U. Koelle, J. Kossakowski, Inorg. Synth. 29 (1992) 225.
[22] U. Koelle, J. Kossakowski, Chem. Commun. 8 (1988) 549.
[23] SMART & SAINT Software Reference Manuals, version 6.22, Bruker AXS Inc.: Madison, WI, 2000.
[24] G.M. Sheldrick, SADABS software for empirical absorption correction, University of Göttingen, Germany, 2000.
[25] SHELXTL Reference Manual, version 5.1, Bruker AXS Inc., Madison, WI, 1998.